remote sensing

MDPI

Article

Spatial–Temporal Analysis of Greenness and Its Relationship with Poverty in China

Wentong Xie [1,2], Yong Ge [1,3,4,5,6,*], Nicholas A. S. Hamm [2], Giles M. Foody [7] and Zhoupeng Ren [8]

1 Institute of Geographic Sciences and Natural Resources Research, Chinese Academy of Sciences, Beijing 100101, China; xiewt@igsnrr.ac.cn
2 School of Geographical Sciences and Geospatial Research Group, Faculty of Science and Engineering, University of Nottingham, Ningbo 315100, China; nicholas.hamm@nottingham.edu.cn
3 Key Laboratory of Poyang Lake Wetland Watershed Research Ministry of Education, Jiangxi Normal University, Nanchang 330022, China
4 Key Laboratory of Natural Disaster Monitoring, Early Warning and Assessment of Jiangxi Province, Nanchang 330022, China
5 School of Geography and Environment, Jiangxi Normal University, Nanchang 330022, China
6 University of Chinese Academy of Sciences, Beijing 100049, China
7 School of Geography, University of Nottingham, University Park, Nottingham NG7 2RD, UK; giles.foody@nottingham.ac.uk
8 State Key Laboratory of Resources and Environmental Information System, Chinese Academy of Sciences, Beijing 100101, China; renzp@lreis.ac.cn
* Correspondence: gey@igsnrr.ac.cn

Abstract: Ecological environmental protection and poverty alleviation are of great significance for the study of human–land relationship coordination and sustainable development, and they have also been a focus of attention in China in the past few decades. In this study, we chose 13 contiguous poverty-stricken areas in China as the study area. Using MODIS Leaf Area Index (LAI) data from 2000 to 2020, the spatial–temporal changes in greenness were obtained using the Bayesian spatial–temporal model (BYM). Spatial autocorrelation was used to identify the spatial distribution of poverty using socio-economic statistical data. Driving factors, including natural factors, poverty factors, and the Grain for Green Policy (GTGP), and their influence on greenness were analyzed by using the Geodetector model for detecting spatial differentiation and factors' interactions. The results showed the following: (1) In 13 contiguous poverty-stricken areas (CPSAs) in China, 59% of the area presented an increasing trend of greenness. (2) In 2000, the high poverty levels with larger MPI values were widely distributed. After 20 years, the overall MPI value was lower, except in some northwest regions with increased MPI values. The spatial autocorrelation of poverty, which relates to the mutual influence of poverty in adjacent areas, also decreased. (3) In the study area, 65.24% of the regions showed strong synergistic effect between greening progress and poverty reduction in the interaction between poverty status and green development. With the improvement of greenness level, the positive correlation between poverty alleviation and ecological environment improvement has become increasingly close. (4) The impacts of interaction factors with the highest q values changed from temperature interacting with precision to regional division interacting with the Grain for Green Policy. The conclusions are that from 2000 to 2020, the impact of natural factors, geographical division, and poverty status on greenness has shown a decreasing trend; The effect of the Grain for Green Policy is gradually increasing; At the same time, the interaction and overlapping effects between the Grain for Green Policy and poverty were increasing. Taking into account the needs of ecological environment, poverty alleviation, and rural revitalization, this research provides valuable reference for formulating and implementing relevant policies based on the actual situation in different regions to promote harmonious coexistence between human-land relationship.

Keywords: greenness; geostatistics; poverty-stricken areas; driving factors

Citation: Xie, W.; Ge, Y.; Hamm, N.A.S.; Foody, G.M.; Ren, Z. Spatial–Temporal Analysis of Greenness and Its Relationship with Poverty in China. *Remote Sens.* **2024**, *16*, 3938. https://doi.org/10.3390/rs16213938

Academic Editors: Jun Yang and Yuji Murayama

Received: 14 August 2024
Revised: 10 October 2024
Accepted: 12 October 2024
Published: 23 October 2024

1. Introduction

The quality of the environment is a major concern and central to international priorities such as the United Nations Sustainable Development Goals (SDGs) [1]. Some studies have used vegetation greenness as a proxy variable for environmental quality and sought to identify and explain the drivers of greenness changes at the regional to global scale with a series of ecosystem models [2,3]. Due to differences in development level and natural environmental conditions, the greening status varies among countries and regions [4]. In harsh environment areas, sensitivity to global climate change, strong spatial–temporal vitality, and heterogeneity are their main characteristics. There are also many studies focused on socio-economic issues in places with harsh environments, especially poverty issues. Since the 1980s, issues of the environment and poverty and the mutual influence between these two factors have already been widely recognized [5]. Previous studies have indicated the existence of a "downward spiral" relationship between regional poverty conditions and environmental degradation [6,7]. There are several classical theoretical models that examine the interrelationship between environment and poverty applied in Tanzania in Africa as an example [8]. However, most studies in Africa or South America are relatively limited by single natural environmental conditions; China has diverse and complex natural geographical conditions. Most of China's ecologically fragile areas are located in transitional areas of ecology and vegetation, with prominent environmental problems, a backward economy, and poor living conditions. Due to these restrictions, the development in these areas has been limited, leading to high poverty levels [9].

Because of the limited resources in poverty-stricken areas in China, the balance between making a living and environmental protection needs to be assessed, and sustainable development measures need to be taken seriously. In recent decades, a lot of measures have been carried out for vegetation restoration (e.g., Grain for Green Policy, Natural Forest Protection Project) and poverty alleviation (targeted poverty alleviation policy). The Grain for Green policy was developed to make efforts to protect and improve the ecological environment and to stop farming on land that is unsuitable for agricultural work. Except for the primary target of reducing ecological environmental degradation, the goals associated with the Grain for Green policy were to promote local socio-economic development [10]. Most ecologically fragile areas in China are in the west, where three-quarters of cropland has a slope > 25°, and 60% of the people living there struggle under the poverty line [11]. Therefore, it is necessary to evaluate the effect of the Grain for Green Policy in China's poverty-stricken areas. The Poverty Alleviation Office of the State Council, an agency established by the Chinese government specifically to address poverty problems, issued the *Outline for Development-Oriented Poverty Reduction for China's Rural Areas* and began to put forward and vigorously implement the targeted poverty alleviation policy in 2013 [12]. In recent years, poverty has decreased, and vegetation protection and restoration have increased in China. However, weak circumstances existed between protecting vegetation and increasing agricultural production and income. Hence, environmental improvement and poverty alleviation have different perspectives that need to be considered. This work aims to study and reveal the changes experienced by the national-level ecological environment, poverty status as well as their related influencing factors, over the past two decades. It is necessary to establish whether this relation is synchronous and to identify the driving factors [13].

Certain socio-economic activities that relate to poverty or support poverty alleviation, such as agricultural production, community construction, forestry management, and vegetation cover changes, can be directly observed through changes in greenness. Vegetation greenness is not only a representation of the ecological environment but also a reflection of human living quality and standards. On a large scale, in the whole of China, the relatively rich areas, such as the southeast coast of China, the Yangtze River Delta, the Pearl River Delta, etc., have relatively high vegetation greenness values. However, the greenness in underdeveloped areas such as Northwest China and the Qinghai–Tibet Plateau is relatively

low. On a small scale, taking residential areas as an example, the greening degree of residential areas where high-income people live is better than that where low-income people live. Some researchers have studied the relationship between vegetation, green space, income health, and well-being [14]. For instance, the vegetation coverage in a residual area could be a predictor for the relative living condition. Known as the "grey-green divide", the number of trees and green space could be regarded as an indicator of the communities' level of the residential areas with different incoming groups. In contrast, higher-income neighborhoods tend to have more greenness in the form of trees and landscaping that show as greening in remotely sensed images. The disparity could be evident when viewing a lower-income residential area that backs into a wealthier one [15]. Therefore, greenness is used as an intuitive representation of vegetation status to describe the condition of the ecological environment, and then further research is conducted on the relationship between vegetation spatiotemporal distribution and poverty.

For the manifestation of greenness, several indexes, including NDVI, LAI, and EVI, were used to estimate vegetation. They were commonly utilized due to their simplicity in calculation based on surface reflectance in optical spectral bands [16]. However, it is important to note that NDVI is a spectral vegetation index, not a biophysical variable. Its drawback is its limited accuracy at places with high LAI values [17]. EVI is an enhancement over NDVI. Compared to NDVI and EVI, the ecological significance of LAI is more pronounced. LAI is defined as the one-sided green leaf area per unit of ground area in broadleaf canopies. For coniferous canopies, it is defined as one-half the total needle surface area per unit of ground area. So, the Leaf Area Index (LAI) is widely used as a proxy for measuring vegetation greenness [2]. The Besag–York–Mollie (BYM) model is a Bayesian model that models spatial, temporal, and local variation. Based on the characteristics of China's ecological and geographical environmental change and the spatial agglomeration and distribution of poverty in locations with harsh natural environments, an understanding of their coupling relationship can be developed by following the research on the vitality of vegetation greenness. Concepts of trade-off and synergy have been widely applied in human–land relationships and ecosystem services studies [18]. This can help to assess whether poverty and ecological protection and restoration measurements are interdependent. When combined with a difficult physical environment (geography, climate, terrain, etc.), the administrative division of continuous poverty-stricken areas, and the regional implementation of policies, the research on poverty should extend from the traditional household level to the regional level. The households in such regions are more likely to fall into persistent poverty, thus forming a spatial poverty agglomeration, which can be identified using local indicators of spatial association (LISA). These methods have emerged as indispensable tools for analyzing spatial patterns and dependencies within datasets [19–22]. The method used for modeling, Geodetector, detects spatially stratified heterogeneity and identifies driving factors [23]. There are four geographical detectors within it, including a risk detector, factor detector, ecological detector, and interaction detector. Researchers have explored applications of the Geodetector model in emerging areas, such as climate change modeling, environment-influencing factors analysis, infectious disease surveillance, and urban resilience planning. Spatial heterogeneity in poverty has not been evaluated previously; hence, there was a lack of information that could explain the interdependence relationships between greenness and poverty. Therefore, we used the poverty change with space–time as one manifestation factor in this work. This is helpful for evaluating the spatial–temporal interdependence relation between greenness and poverty.

Previous work showed that global greening results mainly from CO_2, climate change, nitrogen deposition, and land cover [2]. However, these studies only analyzed natural influencing factors, and there are still unexplained parts in their results that may relate to human activities and policy. Shuai et al. [8] studied the coupling between poverty and the environment, but there is a lack of country-level studies from a whole strategic aspect. Research in related fields, especially some studies on poverty, mainly focuses

on the social science perspective. Therefore, the study presented here addresses the relationships between poverty, environment, and policy for poverty-stricken counties across the whole of mainland China. Our approach is based on geographic information science (GIS). The data are from Earth observation and socio-economic statistical datasets, and the analysis methods are based on recent developments in spatial analysis and spatial statistics.

The aim of this paper is to quantify greenness spatial–temporal change in CPSAs in China and to explore the pattern and relationship between poverty and greenness from 2000–2020. To achieve this, this study will answer the following questions: (1) What are the spatial–temporal changes in greenness in poverty-stricken areas from 2000 to 2020 in China? (2) How did the poverty condition change from 2000 to 2020 in poverty-stricken areas in China? (3) What is the relationship between poverty conditions and greenness during 2000–2020? (4) What are the driving factors, and how do they affect greenness? These objectives are based on existing research on the global trend of vegetation greenness change and poverty socio-economic issues under the Chinese targeted poverty alleviation strategy. It focuses on poverty-stricken areas in China with natural environmental and socio-economic characteristics, comprehensively exploring the spatial–temporal changes in vegetation greenness and regional poverty status in these unique research areas. It explores whether there is a mutually reinforcing state or negative impact between the two issues and explores the influence of various factors such as nature, socio-economic, and policy behind the phenomenon. This has important practical significance for China's major national strategic task in poverty alleviation and the implementation of ecological and environmental protection goals, which is also consistent with the SDGs of UNDP.

2. Materials and Methods

2.1. Study Area

Since concentrated poverty alleviation for contiguous poverty-stricken areas launched in 2011, Chinese governments enforced policies and projects that were regarded as important goals and national development tasks [12]. After the promulgation of the *Outline for Development-Oriented Poverty Reduction for China's Rural Areas (2011–2020)* in 2012 [12], 14 continuous poverty-stricken areas (CPSAs) were delimited, as shown in Figure 1. Among all these areas, Tibetan ethnic areas in Sichuan Province, the southern area of Xinjiang Uygur Autonomous Region, Gansu Province, Yunnan Province, and Qinghai Province have already been targeted with special support policies before 2011 [22]. The other CPSAs were determined according to physical geography, climate, traditional industries, cultural customs, and poverty-causing factors. In total, the CPSAs contain 680 counties in China, and its area covers approximately 3,920,000 km^2. Eighty-six percent of the regions in the CPSAs [24] are in mountainous and hilly areas. These areas are also key ecological environmental protection areas, and almost 40% of people living in poverty live in ecologically fragile areas [25]. In December 2010, 25 key ecological function areas were delimited in the National Main Functional Area Planning [26], which contained 676 counties by the end of 2016, with 378 counties of these 676 counties accounting for 55.9% of the poverty-stricken areas [26]. In this study, we focused on thirteen CPSAs as study areas, excluding Tibet, since there is a lack of continuous and complete time-series data on the region there.

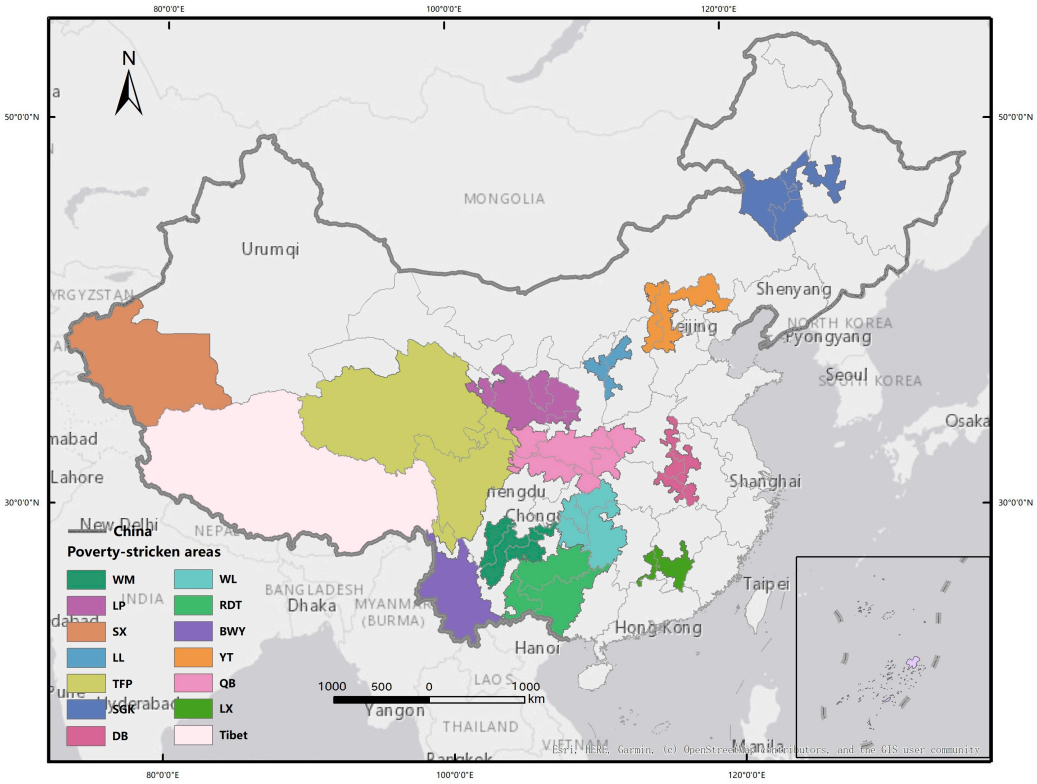

Figure 1. Study area. Fourteen poverty-stricken areas in China. WM—Wumeng; LP—Liupan; SX—south area of Xinjiang; LL—Lvliang; TFP—Tibetan area of four provinces; SGK—south area of Great Khingan; DB—Dabie; WL—Wuling; RDT—rocky desertification of three provinces; BWY—border area of western Yunnan; YT—Yanshan–Taihang; QB—Qinba; LX—Luoxiao.

2.2. Data and Framework

Leaf Area Index (LAI) data used in this study were from MCD15A3H V6 level 4. This product is a 4-day composite dataset with 500 m pixel size. The algorithm for this data product chooses the "best" pixel available from all the acquisitions of both MODIS sensors located on NASA's Terra and Aqua satellites within the 4-day period (https://doi.org/10.5067/MODIS/MCD15A3H.006 (accessed on 4 September 2021)). We collected the data product from Google Earth Engine and calculated the annual average value of each year.

The meteorological data used were the annual mean values for temperature and precipitation. These are gridded data products from the Chinese Academy of Sciences Data Center for Resources and Environmental Sciences (RESDC). They were generated based on the interpolation of daily observation data from more than 2400 meteorological stations. The DEM dataset is from the SRTM (Shuttle Radar Topography Mission) version 4.1, which was resampled to 500 m spatial resolution and downloaded from RESDC [27].

China's Multi-Period Land Use Land Cover Remote Sensing Monitoring Dataset was used as the land use data (CNLUCC) [28]. It was established with the support of the Chinese Academy of Sciences, the national science and technology support program, and other major projects after years of accumulation. Data production is based on Landsat TM/ETM remotely sensed images, which are the main data sources. This study used the first level of classification of the system, which contains farmland, forestland, grassland, water, construction land, and unused land, with a 1 km spatial resolution.

The Resource and Environment Science and Data Centre, Institute of Geographic Sciences and Natural Resources Research, CAS (http://www.resdc.cn/ (accessed on 10 November 2021)), was the data source of meteorological data and land use data used in this work. DEM data were collected from multiple sources to cover this study's time period, considering that the DEM in parts of the country changed significantly over time. Socio-economic data used in this study were gathered from the China Statistical Yearbook (county-level) (https://data.cnki.net/Yearbook (accessed on 10 December 2021)). Statistical data, including per capita GDP, proportion of tertiary industry, number of teachers per 10,000 people, number of medical beds per 10,000 people, per capita housing area, per capita output of grain, and per capita farmland area, were collected for each poverty-stricken county. We aggregated all raster data, including LAI, meteorology, and DEM data, to each county level with the mean value using the zonal statistic tool of ArcGIS so that it could be consistent with county-level units of socio-economic statistical data. The data descriptions are shown in Table 1. Zhao et al. created a relevant research framework on vegetation viability and power transition in rocky specification areas [18], which serves as an important reference and has been further developed in our work. The spatial–temporal analysis method in our framework is the more complicated BYM method. Multidimensional poverty index is used to characterize the comprehensive poverty status, and based on this, LISA clustering map is used to represent the spatial–temporal pattern changes of its poverty status, and a more detailed sub-classified space–time variation has been carried out. Furthermore, Grain for Green Policy, multidimensional poverty status, as well as natural factors were analyzed in the contiguous poverty-stricken areas across China. Based on this, a comparison was made before and after 20 years to observe the changes in influencing factors over the past 20 years. Figure 2 shows the framework applied in this study.

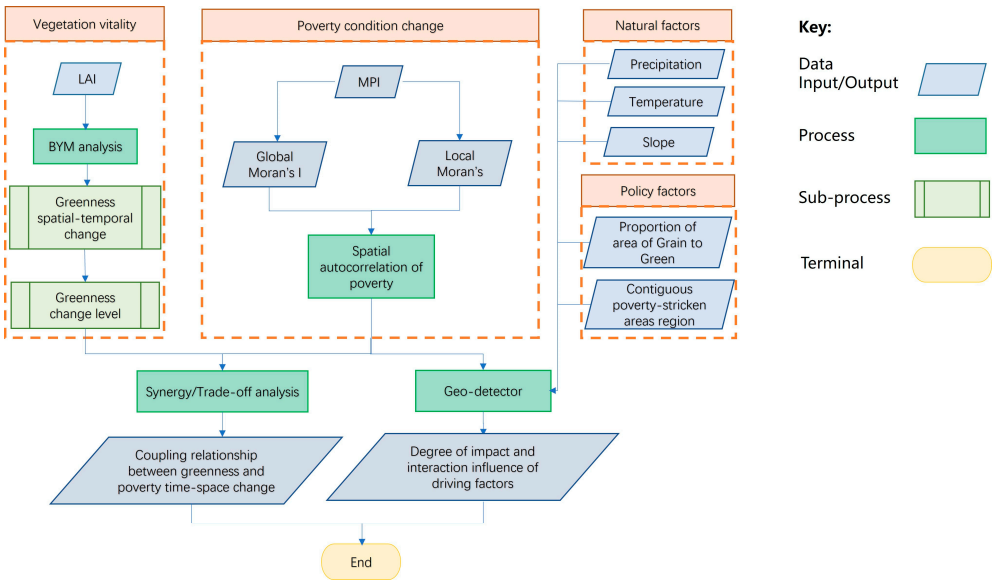

Figure 2. Framework of this study [18].

Table 1. Datasets used in this work.

Data	Description with Source	Resolution	Period	Data Acquisition Platform	
Contiguous poverty-stricken areas in China	Fourteen contiguous poverty-stricken areas (CPSAs) were delimited in 2012 after the promulgation of the *Outline for Development-Oriented Poverty Reduction for China's Rural Areas* (2011–2020) [12]	Counties	2012	Poverty Alleviation Office of the State Council	http://www.gov.cn/gzdt/2012-06/14/content_2161045.html (accessed on 2 May 2020)
Annual LAI	MCD15A3H.006 MODIS Leaf Area Index/FPAR 4-Day Global [29]	500 m	2000–2020	Google Earth Engine	https://developers.google.com/earth-engine/datasets/catalog/MODIS_006_MCD15A3H (accessed on 4 September 2021)
Annual mean temperature	Spatial interpolation data of annual mean temperature [30]	1 km	2000–2020	Resource and Environment Science and Data Center	http://www.resdc.cn/DOI),2022.DOI:10.12078/2022082501 (accessed on 10 November 2021)
Annual mean precipitation	Spatial interpolation data of annual mean precipitation [30]	1 km	2000–2020	Resource and Environment Science and Data Center	http://www.resdc.cn/DOI),2022.DOI:10.12078/2022082501 (accessed on 10 November 2021)
DEM	Produced by SRTM (Shuttle Radar Topography Mission) [31]	500 m	2000	Resource and Environment Science and Data Center	https://www.resdc.cn/data.aspx?DATAID=123 (accessed on 10 November 2021)
	ASTER GDEM produced by METI and NASA [32]	30 m	2005	Geospatial Data Cloud Site, Computer Network Information Center, Chinese Academy of Sciences	https://www.gscloud.cn/ (accessed on 10 February 2022)
	COP-DEM produced by ESA [33]	30 m	2015	National Earth System Science Data Center	https://www.geodata.cn (accessed on 18 February 2022)
	NASA DEM missing data within SRTM was refined with ASTER GDEM elevations [34]	30 m	2020	National Aeronautics and Space Administration (NASA)	https://www.gislounge.com/updated-global-elevation-data-released-by-nasa/?amp (accessed on 10 February 2022)
Land use	The Landsat TM/ETM+ remote sensing images of each period were used as the main data source, which are generated by manual visual interpretation [28]	1 km	2000, 2005, 2010, 2015, 2020	Resource and Environment Science and Data Center	http://www.resdc.cn/DOI,2018.DOI:10.12078/2018070201 (accessed on 10 November 2021)
Socio-economic	Statistical data on the basic situation, economy, agriculture, industry, education, health, and social security of counties in China	Counties	2000–2020	China Socio-economic Big Data Research Platform	https://data.cnki.net/Yearbook (accessed on 10 December 2021)

2.3. Methods

2.3.1. Spatial–Temporal Changes in Greenness

We adopted the Besag–York–Mollie (BYM) model [27]. This is a hierarchical Bayesian model that accounts for the spatial and temporal dependency in areal data. The advantage of this model is its flexibility in incorporating an overall spatial structure while allowing temporal dependence to vary in space and time. We used this model to identify the spatial–temporal change pattern of LAI from 2000 to 2020 [35]. We assumed that the LAI for each county followed normal distribution, which is supported by the histograms generated for the MODIS LAI values at a resolution of 500 m in all poverty-stricken areas and counties (Figure S1). In the model, y_{it} represent the annual average value of LAI in ith county at tth year.

$$y_{it} \sim Normal\left(\mu_{it}, \sigma^2\right) \quad (1)$$

μ_{it} can be modeled as follows:

$$\mu_{it} = \alpha + s_i + b_0 t + v_t + b_{1i} t \quad (2)$$

During this modeling, the observed space–time variability of greenness condition is decomposed into the following components [22]. The spatial coefficient, s_i, describes the stability of the spatial pattern of the entire study area during a 20-year observation period. $b_0 t + v_t$ represents the trend over the twenty years in the whole study area. The overall time trend is decomposed by a linear function ($b_0 t$) with an additional term (v_t), which allows for nonlinearity in the overall trend pattern [36,37]. The stable component of greenness change was represented by combining the common spatial pattern and the common time trend together. The term $b_{1i} t$ allows each county to have its own change trend. While b_0 is the overall rate of change in greenness change, b_{1i} measures the departure from b_0 for each county. For instance, a negative value of b_{1i} indicates a declining trend in greenness change over time, and α is the intercept term [38]. We adopted non-informative prior distributions of all parameters, with the precise implementation being described in the Supporting Materials [35]. The model was implemented using the OpenBUGS 3.2 (https://openbugs.net/ (accessed on 12 August 2024)) software, which is specially designed for Bayesian analysis [39]. See Supporting Materials for code.

2.3.2. Multidimensional Poverty Index

There are multiple dimensions to quantify poverty. Income was the most widely used poverty standard in the world before 1990. In 2010, the United Nations Development Programme's Human Development Report further released a multidimensional poverty index (MPI) based on Alkire et al. [40]. The multidimensional poverty index (MPI) is an aggregate index that quantifies the poverty phenomenon with multiple indicators, including education, health, and living standards [40]. International research and indicator construction on poverty issues are usually carried out from three aspects: economy, society, and nature [41,42]. In this study, as we explored not only socio-economic conditions but also linked them to the living environment, we set the three dimensions as economy, society, and the environment with seven indicators across these three dimensions, which can be observed and collected as shown in Table 2.

The evaluation indicators can be divided into positive indicators and negative indicators. For positive indicators, the larger the value, the better, while for negative indicators, the smaller the value, the better. Due to the different dimensions and units of each evaluation indicator, they are not comparable. In order to eliminate the incompatibility between indicators, it is necessary to normalize the dimensions of the evaluation indicators. This study adopted the range normalization method to convert the numerical values to values between 0 and 1. The equation for a positive indicator is as follows:

$$X'_{ij} = \left(X_{ij} - min\{X_j\}\right) / \left(max\{X_j\} - min\{X_j\}\right) \quad (3)$$

The equation for a negative indicator is

$$X'_{ij} = \left(max\{X_j\} - X_{ij}\right) / \left(max\{X_j\} - min\{X_j\}\right) \quad (4)$$

X'_{ij} is the standardized data, X_{ij} is the jth index of the ith spatial unit, and $max\{X_j\}$ and $min\{X_j\}$ are the maximum value and minimum value of the j index.

Table 2. Indicators used for the multidimensional poverty index (MPI) for this study.

Dimension	Index	Unit
Economy	Per capita GDP	10 thousand RMB/person
	Proportion of tertiary industry	%
Society	Number of teachers per 10,000 people	Person/10,000 people
	Number of medical beds per 10,000 people	Person/10,000 people
	Housing area per capita	m^2/person
Environment	Per capita output of grain	kg/person
	Farmland area per capita	ha^2/person

Since the impact of different indicators on poverty is not the same, it is necessary to determine the weight of each indicator [43]. This paper used combination of equal weight method and entropy method to determine the weight of indicators. The equal weight method is used for the weights of economic development, social development, and environmental development, with each dimension set at 1/3 [44]. The weight, w_j, of different indicators in each dimension was calculated by the entropy method, and the process is as follows. Calculate the proportion P_{ij} of the index value of the ith space unit under the jth index:

$$P_{ij} = X'_{ij} / \sum_{i=1}^{n} X'_{ij} \quad (5)$$

The entropy value e_j and the index difference coefficient g_j are given as follows:

$$e_j = (-1/\ln n) \times \sum_{i=1}^{n} P_{ij} \ln P_{ij} \quad g_j = 1 - e_j \quad (6)$$

The weight of the indicators is

$$w_j = g_j / \sum_{j=1}^{m} g_j \quad (7)$$

The score of each dimension was calculated and then added to obtain the multidimensional poverty index.

$$\begin{aligned} E_i &= \sum_{i=1}^{n} \sum_{j=1}^{2} X'_{ij} w_j \\ S_i &= \sum_{i=1}^{n} \sum_{j=3}^{5} X'_{ij} w_j \\ N_i &= \sum_{i=1}^{n} \sum_{j=6}^{7} X'_{ij} w_j \\ MPI_i &= E_i + S_i + N_i \end{aligned} \quad (8)$$

where E_i, S_i, and N_i are the scores of economic development, social development, and environmental development, respectively.

2.3.3. Poverty Spatial Pattern and Change Analysis

Moran's I is a spatial autocorrelation statistic calculated for a specific spatial distance. Global Moran's I gives a single statistic for the entire study area, whereas the local Moran's I can be mapped to show the variability across the study area. Local Moran's I is a local indicator of spatial association (LISA) [20,45,46] and identifies clusters of high–high, low–low, high–low, or low–high spatial association. Moran's I is typically given as a z-score, and a p-value is calculated by a permutation to allow the user to evaluate whether the statistic is significantly different from zero. The formula of Global Moran's I is as follows:

$$I = \frac{n\sum_{i=1}^{n}\sum_{j=1}^{n}\omega_{ij}(x_i - \overline{x})(x_j - \overline{x})}{S\sum_{i=1}^{n}(x_i - \overline{x})^2} \quad (9)$$

where n represents the number of spatial units, county, x_i represents the attribute value of the ith spatial unit, and ω_{ij} represents each value in the spatial weight matrix, and the value of S is the sum of all the elements in the matrix. The spatial weights matrix is used to define the local neighborhood. The neighborhood is defined by the user, although a typical neighborhood is the first-order Queen's contiguity neighborhood whereby spatial units that share a boundary or corner are assigned a weight of one, and all other spatial units are assigned a weight of zero. We constructed spatial weights matrix and used the simulation process of permutation-based hypothesis testing. The value range of Moran's I is $[-1, 1]$. A Moran's I index larger than 0 represents positive spatial autocorrelation with the clustered pattern, while an index smaller than 0 indicates a negative spatial autocorrelation with the dispersed pattern. Moran's I index's values close to 0 show that the variables are distributed with random patterns. The local Moran's I is calculated around each spatial unit, i.

The space–time changes in the poverty condition were separated into seven types: $Type_0$, $Type_1$, $Type_2$, $Type_3$, $Type_4$, $Type_5$, and $Type_6$ (Table 3) [47]. This was referenced from the approach that divided space–time transition into four types from Table 2 of the paper from Zhao et al. [18]. On this basis, we have further refined Type4, space–time coagulation into 3 sub-types, the current Type4, Type5, and Type6. Considering the values changes, HH → LL was identified as the space–time coagulation-positive (SC_P) trans due to the poverty condition change from high level to low level; LL → HH was identified as the space–time coagulation-negative (SC_N) trans; HL → LH and LH → HL were identified as the space–time coagulation-irregular (SC_I) trans (Table 3).

Table 3. The types of space–time change for poverty conditions [18].

Type	Description	Evolution	Time and Space Change
Type0	No transition between self and neighbors.	Invariant	Space–time lock (SL) (low level)
Type1	Self-transition, neighbors no-transition	HH → LH, HL → LL, LH → HH, LL → HL	Space–time flow (SF) (middle level)
Type2	Neighbors transition, self no-transition.	HH → HL, HL → HH, LH → LL, LL → LH	
Type3	Self and neighbors transform in the same direction.	HH → LL	Space–time coagulation-positive trans (SC_P) (high level)
Type4		LL → HH	Space–time coagulation-negative trans (SC_N) (high level)
Type5	Self and neighbors transform in the contrary direction.	HL → LH	Space–time coagulation -irregular trans (SC_I) (high level)
Type6		LH → HL	

2.3.4. Relationship Between Greenness Dynamic and Poverty Change

Based on the trend in greenness change, if the estimated value of b_{1i} of BYM model is >0, it is a positive greening trend. If the estimated value is <0, there is a browning trend. The greening level variation was divided into three levels—slow, stable, and quick—according to the natural break method. According to the spatial–temporal changes in poverty, the condition was divided into the following categories: SC (space–time coagulation), SL (space–time lock), and SF (space–time flow), which represent the spatial–temporal poverty change with the high, middle, and low degrees/possibilities. Trade-off and synergy concepts have normally been applied in ecological, human–land relationship research to identify conflicts and benefits [18,48]. Synergy means positive relation between two factors; on the contrary, trade-off is considered a negative relation. In this work, the relationship between greenness spatial–temporal patterns and poverty was assessed. We classified and combined the

changes in greenness and spatial clustering of poverty for each category and determined the trade-off or synergy relationship categories based on a series of combinations referencing Table 3 from the paper of Zhao et al. [18]. The coupling relationships between greenness and poverty change are shown in Table 4. Browning with space–time lock (SL) means that when the vegetation coverage decreases negatively, there is no change in the spatial association of poverty. Any greening trend together with space–time lock (SL) was regarded as a trade-off which means that the poverty condition does not change with the greening trend. For the greening trend with different space–time change degrees with space–time flow (SF) and space–time coagulation (SC), it was regarded as a weak and strong synergy. Based on the subtypes divided in Table 3, we categorized them as follows: all the space–time coagulation types, including space–time coagulation-positive trans (SC_P), space–time coagulation-negative trans (SC_N), and space–time coagulation-irregular trans (SC_I), are regarded as strong synergy.

Table 4. The coupling relationship of greenness and poverty change [18].

Greenness Change Level	Poverty Changes Type	Trade-Off and Synergy
Browning	Space–time lock (SL)	Trade-off
	Space–time flow (SF)	Weak synergy
	Space–time coagulation (SC)	Strong synergy
Slowly greening	Space–time lock (SL)	Trade-off
	Space–time flow (SF)	Weak synergy
	Space–time coagulation (SC)	Strong synergy
Stable greening	Space–time lock (SL)	Trade-off
	Space–time flow (SF)	Weak synergy
	Space–time coagulation (SC)	Strong synergy
Quick greening	Space–time lock (SL)	Trade-off
	Space–time flow (SF)	Weak synergy
	Space–time coagulation (SC)	Strong synergy

2.3.5. Quantifying the Grain for Green Policy

The Grain for Green Policy has an important influence on the greenness of China's poverty-stricken areas, so it is essential to quantify its influence. The most important point of this policy is to convert the farmland that is not suitable for cultivation into forestland. Therefore, the method adopted in this study was to quantify the implementation area proportion of Grain for Green Policy in each county by using the changes in land use type and overlaying the slope range that is not suitable for agricultural activities [49].

A Markov model is a kind of stochastic process. It can predict the next state of events and its change trend through the initial probability of different states of events at each time and the transfer relationship between states. It has been widely used in land use change prediction and simulation [50]. The Markov model for land transfer matrix operates on the principles of transition probabilities between discrete land cover categories, adhering to the first-order Markov property where future states depend solely on the current state. It utilizes a transition matrix to quantify the likelihood of transitioning between land cover classes within a specified time frame. The formula is as follows:

$$S_{(t+1)} = P_{ij} \times S_t \tag{10}$$

$$s_{ij} = \begin{matrix} s_{11} & s_{12} & s_{13} & \dots & s_{1n} \\ s_{21} & s_{22} & s_{23} & \dots & s_{2n} \\ s_{31} & s_{32} & s_{33} & \dots & s_{3n} \\ \dots & \dots & \dots & \dots & \dots \\ s_{n1} & s_{n2} & s_{n3} & \dots & s_{nn} \end{matrix} \quad (i, j = 1, 2, 3, \dots n) \tag{11}$$

$S_{(t+1)}$ and S_t represent the land use statuses of the $t+1$ and t periods, respectively. P_{ij} is the transition probability of type i to type j. S_{ij} is the area of type i transformed into type j. n is the number of land use types. i and j are the land use types before and after the transfer. According to Grain for Green Policy, farmland with slope of more than 25° and farmland with an important water source area with a slope between 15 and 25° were chosen as the Grain for Green Policy implementation area [51]. The slope calculated by DEM datasets and the results of the land transfer matrix are overlapped to calculate the proportion of the area of farmland converted into forestland in each county within the specified slope range.

2.3.6. Geodetector: Driving Factors Influencing Greenness Change

The Geodetector is the method that is utilized to detect the interactions between different driving factors by calculating the variances in space [23]. It is a statistical method to evaluate spatial heterogeneity in a target variable and quantify the driving forces behind it. Its core idea is that if a predictor variable has a significant influence on the response variable, then the spatial distribution of both variables should be similar. Geodetector has applications across various disciplines, including epidemiology, ecology, transportation planning, and regional development, highlighting its versatility and broad utility in spatial analysis. The response variable and the covariates (termed driving variables or factors) are divided into spatial categories, also called strata. The objective is to compare the within-strata variance to the between-strata variance. Geodetector has the advantage of handling both numerical and categorical variables based on the characteristics of each district. It can detect the interaction between two factors on the dependent variable, which helps explain the phenomenon affected by multiple complex effects, and its results are not affected by multivariate collinearity. There are four geographical detectors with Geodetector, including risk detector, factor detector, ecological detector, and interaction detector [23]. The factor detector is used to quantify the influence of each variable individually, whereas the interaction detector is used to study the interaction between pairs of factors.

The factor detector makes use of the q-statistic. This quantifies the spatially stratified heterogeneity of the response variable. Alternatively, it measures the influence of a given covariate on the response variable, which is termed the power of the determinant. The q-statistic is calculated as follows:

$$q = 1 - \sum_{h=1}^{L} N_h \sigma_h^2 / N\sigma^2 = 1 - SSW/SST \tag{12}$$

$$SSW = \sum_{h=1}^{L} N_h \sigma_h^2 \tag{13}$$

$$SST = \sum_{i}^{N} \left(Y_i - \overline{Y}\right)^2 = N\sigma^2 \tag{14}$$

The study area is composed of sub-regions, which were regarded as N units and is stratified into $h = 1 \ldots L$ stratum. N_h is the number of units (observations) in strata h, and N is the number of units in the entire domain. Y_i denotes the value of unit i of the variable in the group, and $\overline{Y}$ is the mean value of Y_i. σ_h^2 and σ^2 are the variances in the stratum and the variances in the domain. SSW is the sum of the spatial variance in all strata; SST is the total sum of squares. The value of q ranges from 0 to 1; q value is 0 if there is no stratified heterogeneity, and q value is 1 if the group is fully stratified.

The candidate factors are shown in Table 5. The LAI value of greenness was taken as the response variable y. The predictor variables were selected according to the following factors [52]. The independent variable X_1 is the poverty factor MPI. The independent variable X_2 is mean annual precipitation of the county. The independent variable X_3 is the annual mean temperature of the county. The independent variable X_4 is the mean value of slope of the county. The independent variable X_5 is the contiguous poverty-stricken area. The proportion area of returning farmland to forestland of each county is the independent variable X_6 (Table 5).

Table 5. Variables for Geodetector.

Variable	Name	Name	Description	Category
y	Greenness	LAI value	Using zonal statistic tool to calculate the LAI value of each county	
X_1	Poverty factor	MPI	According to SL and SF classification	
X_2	Natural factors	Annual mean precipitation	Using zonal statistic tool to calculate the average annual precipitation value of every county	6 ranges produced by natural breaks (Jenks) method
X_3		Annual mean temperature	Using zonal statistic tool to calculate the annual mean temperature value of each county	
X_4		Slope	Using zonal statistic tool to calculate the slope value of each county	
X_5	Regional division	13 contiguous poverty-stricken areas (without Tibet)	According to Figure 1, it is divided into 13 categories	Dabie, southern area of Great Khingan, rocky desertification of three provinces, border area of western Yunnan, Liupan, Luoxiao, Lvliang, Qinba, Tibetan area of four provinces, Wumeng, Wuling, southern area of Xinjiang, Yanshan–Taihang
X_6	Grain for Green Policy factors	The proportion of the land area of farmland returning to forest in each county	By calculating the land transfer matrix, the land area converted from cultivated land to forest land in each county is calculated. Combined with the requirements of Grain for Green Policy, the slope cultivated land of more than 25° and the slope cultivated land of 15–25° in the important water source area are superimposed with the slope to calculate the area ratio implemented by Grain for Green Policy	6 ranges produced by natural breaks (Jenks) method

3. Results

3.1. Spatial–Temporal Changes in Greenness in a Contiguous Poverty-Stricken Area in China

The BYM model was used to quantify the overall temporal trend as well as the change trends of each county. The obtained mean of $b_0t + v_t$ is the measurement for the overall temporal change trend for LAI from 2000 to 2020. Figure 3 shows the value of $b_0t + v_t$ over time for LAI and illustrates that the overall temporal change of LAI increased with continuous fluctuations. The overall situation fluctuated around zero between 2000 and 2014 but increased from 2014.

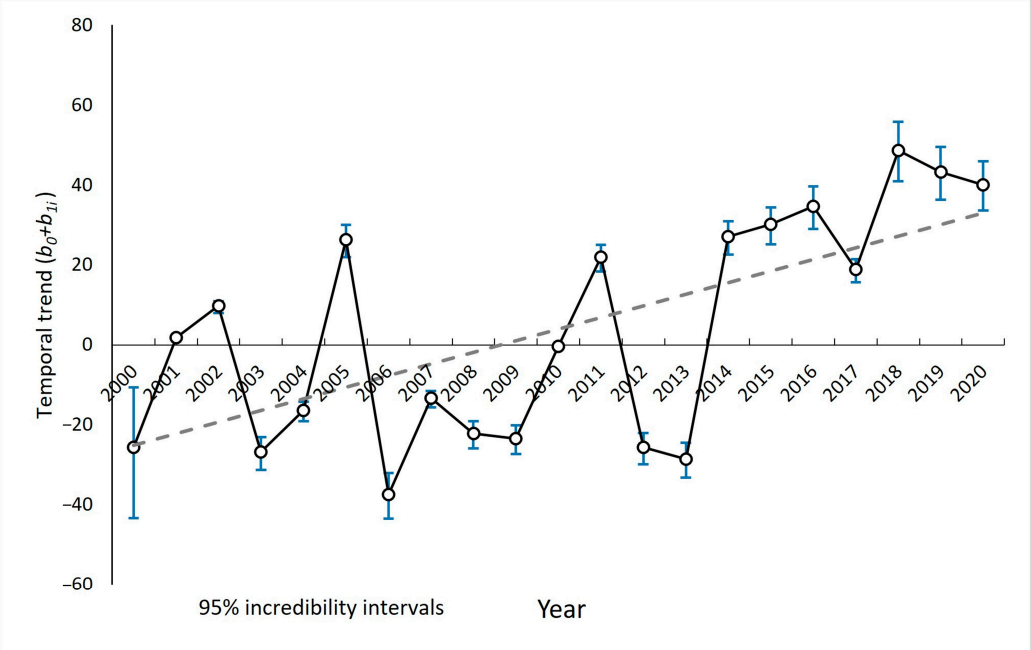

Figure 3. Temporal trend ($b_0 + b_{1i}$) of greenness of poverty-stricken areas in China from 2000 to 2020. The blue vertical line shows the credibility interval for each year.

The obtained posterior median of $b_0 + b_{1i}$ quantifies the change trends for each county locally. A negative value of $b_0 + b_{1i}$ indicates that a decreasing greenness trend for ith county from 2000 to 2020 leads to a more rapid decrease with the lower value. On the contrary, a positive value indicates an increasing trend of the ith county and a more rapid increase with the higher value. Figure 4 maps the $b_0 + b_{1i}$ values. It demonstrates that the south shows the most obvious positive increasing trend, and a small part of southwest and north China showed a negative decrease, while other regions showed a relatively stable small positive increase trend of greenness. The results of this spatial distribution are shown in Figure S2. From 2000 to 2020, the spatial–temporal change result value of greenness in 59% of the impoverished counties was greater than zero; in 35% of the impoverished counties, it was less than zero; and in 6% of the impoverished counties, it was not significantly different from zero. In Lvliang, Luoxiao, and the border area of western Yunnan, more than 90% of the areas in these regions showed a greening trend (Table 6). Among all the continuous poverty-stricken areas (CPSAs), Wuling, the southern area of Xinjiang, and the Tibetan area of four provinces were the ones with the lowest greening trend. The Chinese provinces are illustrated in Figure 1.

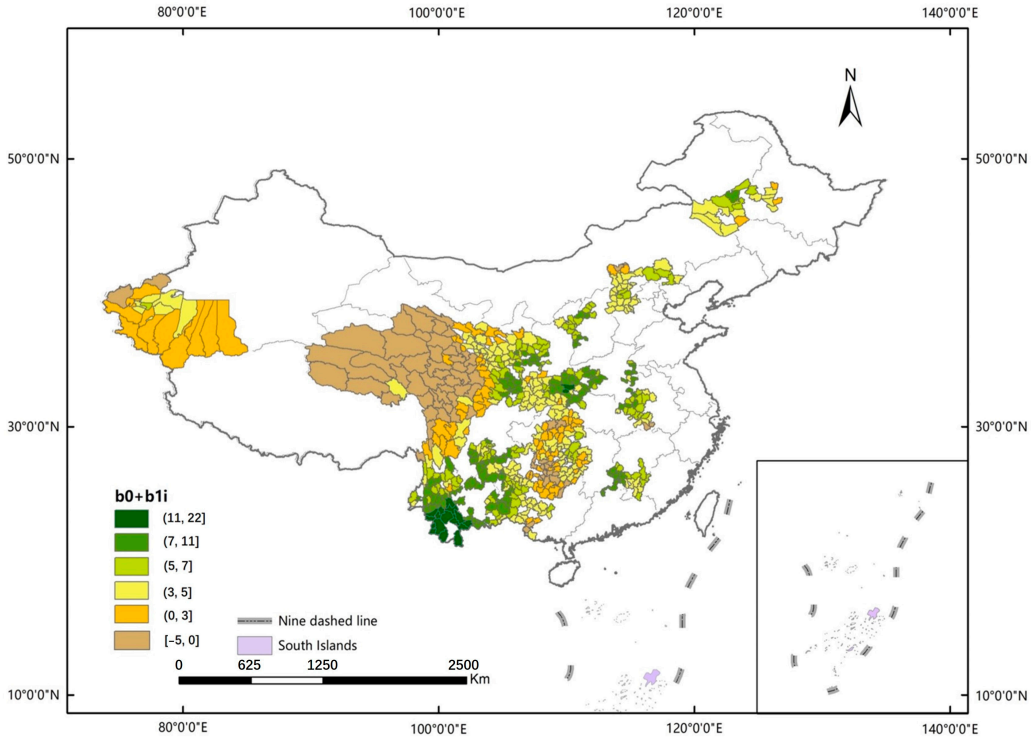

Figure 4. Spatial–temporal changes in greenness. The 6 categories were identified using the natural breaks method.

Table 6. Rank of the proportion of area in CPSA greenness dynamic in different regions.

Rank (High to Low)	The Proportion of Greening Area in the Total Area	Contiguous Poverty-Stricken Area
1	95.00%	LVL
2	94.44%	BWY
3	91.30%	LX
4	80.82%	QB
5	79.41%	DB
6	72.22%	SGK
7	72.22%	WM
8	68.33%	LP
9	63.64%	TY
10	50.00%	RDT
11	30.16%	WL
12	20.83%	SX
13	4.05%	TFP

3.2. Spatial–Temporal Changes in Poverty

The poverty condition shows changed during the period 2000–2020, as shown in Figure 5. According to the spatial distribution of MPI (Figure 5), Figure 5a shows that in 2000, the MPI values greater than 0.3 were widely distributed, especially in the range of 0.5–0.7. In 2005 (Figure 5b), some regions began to show values of MPI > 0.7, mainly distributed in small parts of the northeast and northwest. Based on the results of MPI changes every 5 years, the spatial distribution of MPI varied. Low values were distributed more widely and occupied a larger area. The concentrated and contiguous regional poverty distribution transformed into a scattered distribution. The poverty status in most regions with MPI values between 0.5 and 0.7 gradually eased, and their MPI values gradually remained between 0.1 and 0.3. By 2020, as shown in Figure 5e, the overall MPI value was lower, and most of the CPSA region had maintained a relatively low level of poverty, except

for a small portion in the northwest of the Qinghai–Tibet Plateau where higher MPI values were observed, indicating that there might be a risk of returning to poverty in this area.

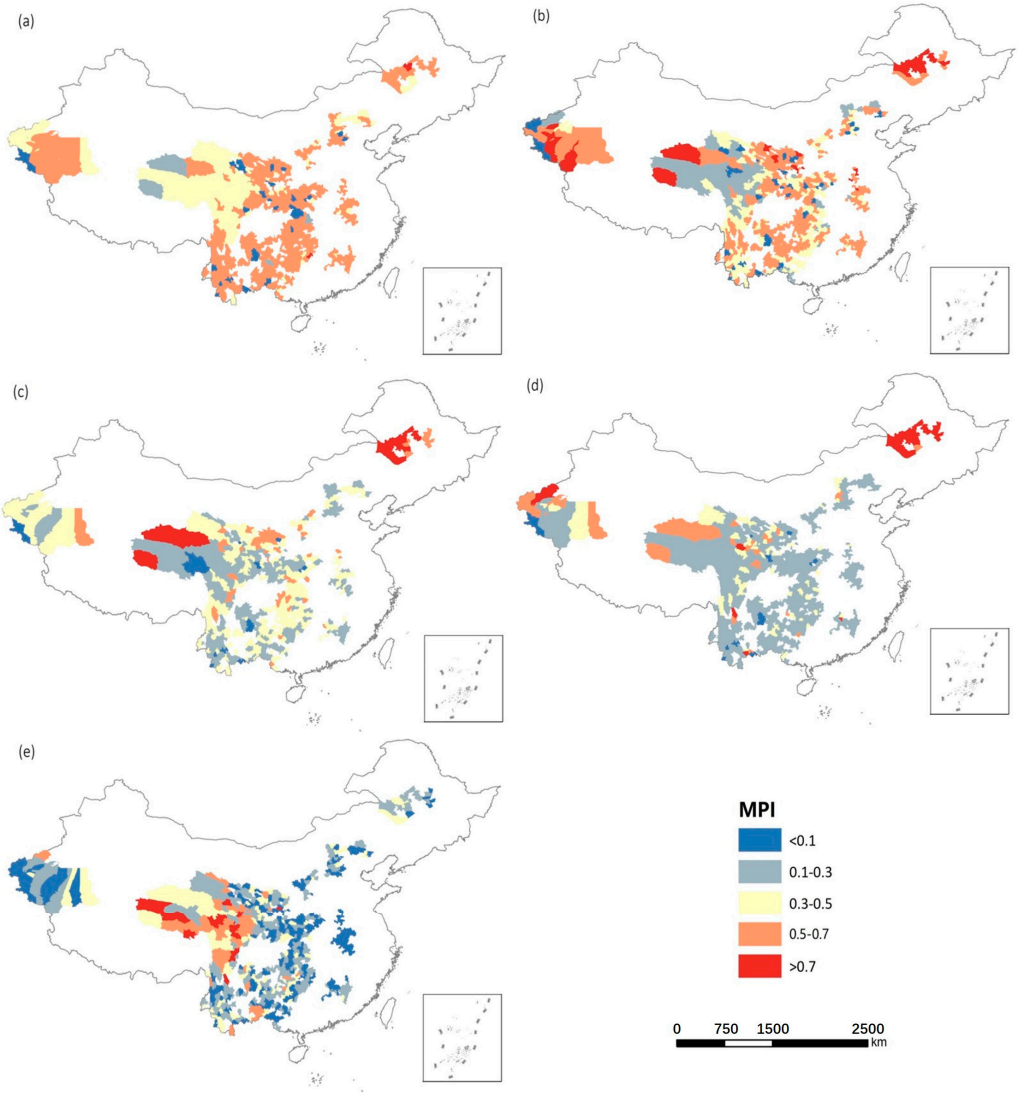

Figure 5. Mapping of MPI. (**a**–**e**) represent the MPI values of 2000, 2005, 2010, 2015, and 2020, respectively.

Based on the implementation process of China's poverty alleviation policies, we can explain the reasons for the results. The poverty-alleviation policy started in the new century in 2000. We learn from Figure 5a that poverty was widespread in contiguous poverty-stricken areas. With the issue of the *Rural Poverty Alleviation and Development Program (2001–2010)* [13], in 2005 and 2010, most of the areas that were originally orange in 2000 turned yellow and light blue, indicating the effectiveness of the policy in improving poverty. In 2013, we entered the stage of targeted poverty alleviation [13], which changed the targets from national and regional levels to village and household levels with specific measures. As shown in Figure 5d, in 2015, except for a few regions in the northwest and northeast, the light blue area had become the majority. However, by 2020 (Figure 5e), we found that in some regions of Qinghai–Tibet Plateau of Northwest China, a small portion of MPI values had increased again, indicating a potential risk of returning to poverty. The reason may be due to the influence of the natural environment, resource endowment, and other institutional constraints. The implementation and effectiveness of poverty alleviation policies in the region are relatively slow, and there may be a certain lag in their effects.

Moran's I measures the spatial autocorrelation relative to neighboring polygons. The global Moran's I result for MPI in CPSAs from 2000 to 2020 is shown in Table 7. During the 20 years, Moran's I results show a fluctuating trend of slight decline, followed by a significant increase and then a further decline. In terms of the magnitude of the changes, the spatial autocorrelation of poverty changed significantly between 2005 and 2010, as well as between 2010 and 2015. In all these cases, the poverty pattern showed clustered conditions. The local Moran's I for MPI is shown in Figure 6. From 2000 to 2020, the number of HH and LL clusters decreased, and the spatial aggregation decreased. By 2020, except for the eastern areas, the country basically did not show the characteristic of poverty clustering.

Table 7. The global spatial autocorrelation results of MPI in CPSAs.

Year	Moran'I	z Value	*p* Value
2000	0.234	8.2659	0.001
2005	0.126	4.4482	0.001
2010	0.775	22.6983	0.001
2015	0.281	21.1388	0.001
2020	0.445	15.0749	0.001

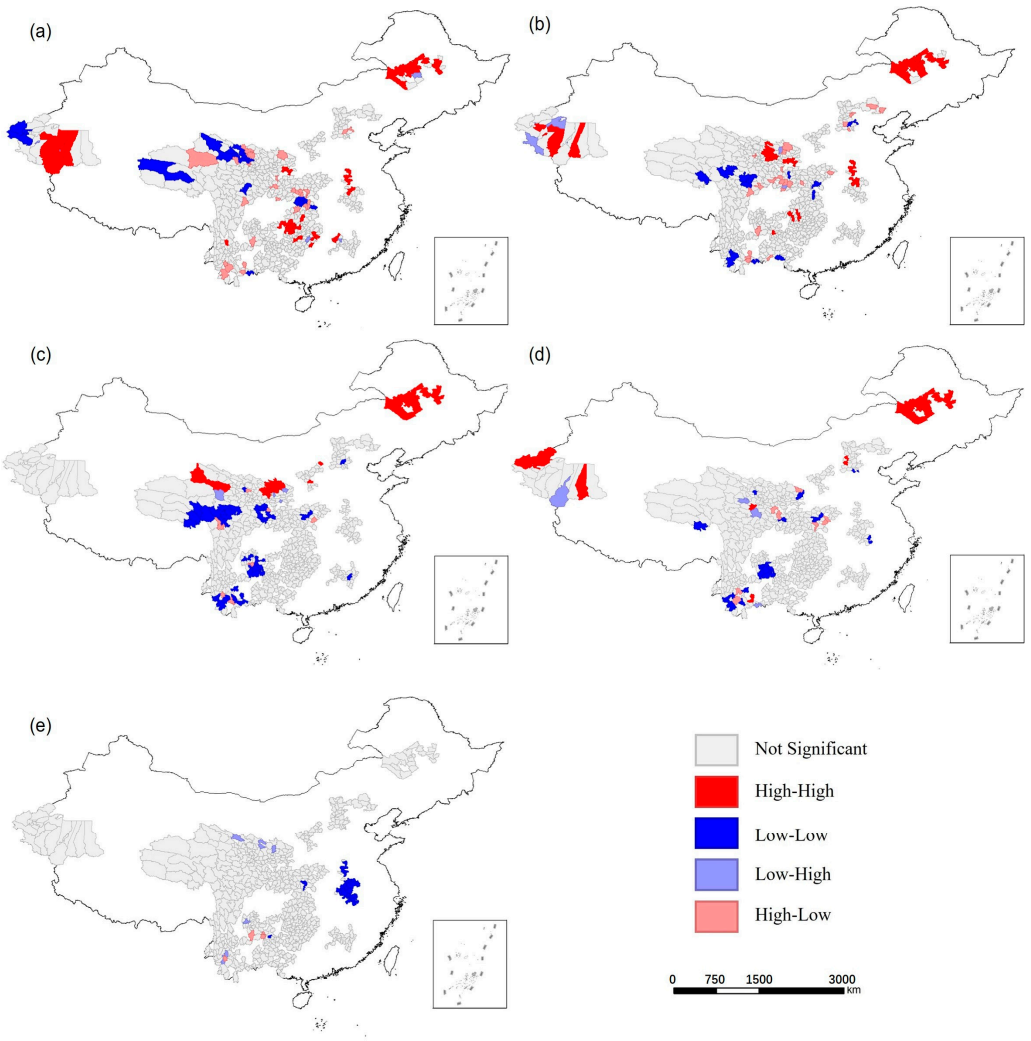

Figure 6. LISA cluster map for MPI. (**a**) 2000; (**b**) 2005; (**c**) 2010; (**d**) 2015; (**e**) 2020.

3.3. Relationship Between Greenness Dynamic and Poverty

For the coupling relationship between poverty and vegetation greenness, we first identified the greenness change level, including browning, slow greening, stable greening, and quick greening, of each county based on the results obtained earlier. Based on the LISA cluster map of MPI for each county from 2000 to 2020 in Figure 6, we matched the corresponding categories of poverty condition changes for each county according to the classification in Table 3 to classify which type the poverty condition change belongs to. Based on the above two results, according to the classification matching rules in Table 4, we can determine whether each county is categorized as trade-off or synergy, as well as the degree of different synergy. In order to present the results clearly, the bar chart was used here to show the proportion of each area, and it is totally referenced by Figure 6 in the paper of Zhao et al. [18]. According to each poverty-stricken area as the scope, calculate the proportion of different coupling relationships in the total area of the poverty-stricken area and obtain Figure S3 as a result. For the whole CPSAs, the area of strong synergies between greenness change and poverty change account for 34.76% (browning), 29.63% (slow greening), 27.59% (stable greening), and 33.64% (quick greening), respectively. However, the area proportion of trade-off between greenness and poverty change was observed by 64.29% (browning), 70.37% (slowly greening), 72.41% (stable greening), and 65.44% (quick greening). Observing all the regions, we found that 33.39% of the study area has synergistic conditions, and 66.61% has trade-off conditions (Figure S3). In general, the larger the change in the greenness condition, the more the proportion of synergy relationship between the greenness trend and poverty change, which can illustrate that the positive greenness condition and the improvement of poverty alleviation have a synergy relationship. We observed that relationships between greenness and poverty varied in space (Figure 7). In terms of the proportion of trade-offs between greenness and poverty change in the southern area of Xinjiang and Lvliang and the rocky desertification of three provinces, Liupan experienced the largest change. In the Dabie, Wumeng, Luoxiao, and Tibetan areas of the four provinces, the opposite was observed (Figure S3).

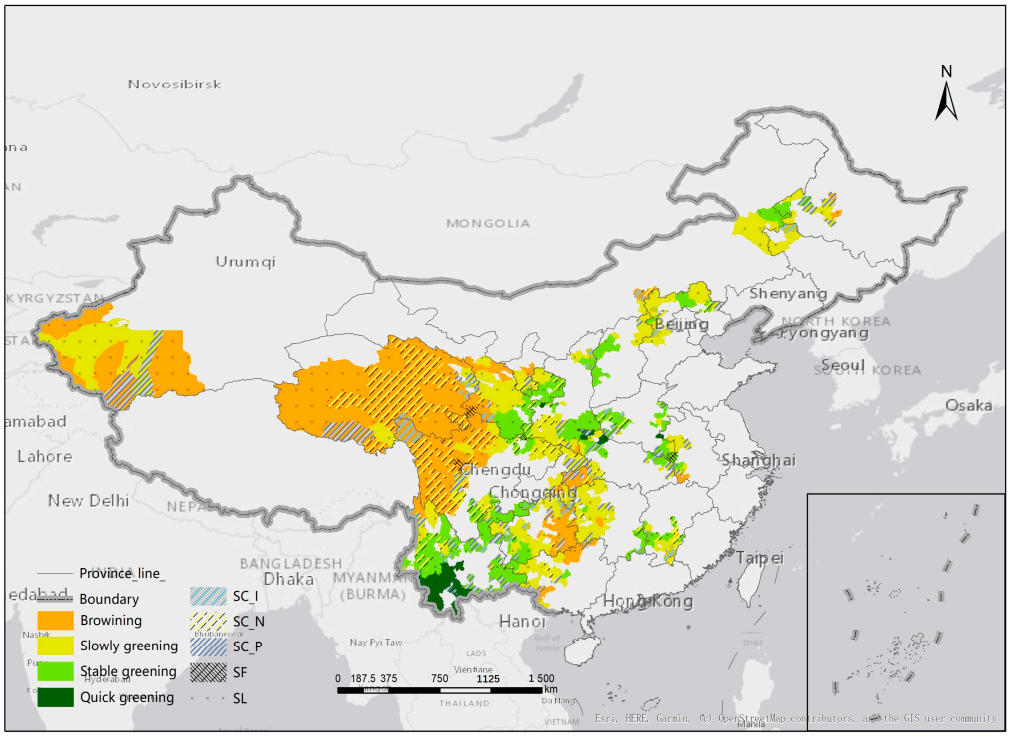

Figure 7. Spatial distribution of the relationship between greenness and poverty changes in CPSAs by dividing browning, slowly greening, stable greening, and quick greening areas.

3.4. Geodetector: The Association of Greenness and Poverty, the Degree of Impact and Mutual Influence

The results of the Geodetector factor analysis are shown in Tables 8 and 9 and show the influence of each hypothesized driving factor on greenness. In 2000, temperature and precipitation had the largest effect. In 2020, the region and Grain for Green Policy had the greatest influence, while temperature and precipitation took second place, and slope had the least influence. Compared with 2000 and 2020, the q value of the region, Grain for Green Policy, and slope increased. The q values of temperature, precipitation, and MPI all decreased (Tables 8 and 9). In the results of interaction analysis within Geodetector, the symbol "∩" represents the intersection operation. Specifically, in the context of Geodetector, it not only analyzed the individual influence of each factor on the observed outcome independently, its interaction analysis, but also examines how combinations of spatial factors interact with each other to collectively influence the observed outcome. This involves assessing the joint effects of multiple factors and identifying whether these interactions significantly impact the outcome.

Table 8. Factor analysis in 2000.

	Region	Grain for Green	Temperature	Precipitation	MPI	Slope
q statistic	0.4189	0.3234	0.6393	0.5475	0.0048	0.0223
p value	<0.001	0.0566	<0.001	<0.001	0.0919	0.0358

Table 9. Factor analysis in 2020.

	Region	Grain for Green	Temperature	Precipitation	MPI	Slope
q statistic	0.7851	0.7534	0.4393	0.3959	0.0013	0.0257
p value	<0.001	0.0496	<0.001	<0.001	0.0919	0.0359

Tables 10 and 11 show that in 2000, the groups of important driving factors that can affect greenness change with importance were Temperature ∩ Precipitation: 0.6665; Regional Division ∩ Precipitation: 0.6107; and Temperature ∩ Slope: 0.6337. In 2020, factor groups including Regional Division ∩ Grain for Green with 0.6568, Grain for Green ∩ Temperature with 0.5112, Grain for Green ∩ Precipitation with 0.5621, and Grain for Green ∩ Slope with 0.5455 have a high degree of influence and interaction relationships. In addition, Regional Division ∩ Grain for Green, Grain for Green ∩ Temperature, and Grain for Green ∩ Slope in 2020 showed a higher q value compared with 2000, which illustrates that these factors have a greater impact on greenness change and enhanced relationships. In CPSAs in China, in addition to the continuity of space and socio-economic conditions, the natural environment is also a very important basis. Each region has its own characteristics of natural environment, especially has different degrees of promotion or restriction on vegetation growth conditions and ecological environment. Therefore, the interaction of regional division with temperature, precipitation, and poverty transition has a greater impact. During the research period, 2010 was the time point for the end of the first round of the Grain for Green Policy, and 2012 was the time point for the start of the second round. The impact of the intersection of MPI and Grain for Green Policy is also relatively large, especially the q value in 2020 is larger than that in 2000. The influence of temperature and precipitation and its interaction with other factors is closely related to vegetation growth, so the q value is larger, but its impact is relatively reduced.

Table 10. The dominant interactions between two covariates on greenness in 2000.

Interaction	Degree of the Relationship (q)	*p* Value
Regional Division ∩ Grain for Green	0.2249 **	0.0249
Regional Division ∩ Temperature	0.5028 **	0.0302
Regional Division ∩ Precipitation	0.6107 ***	0.0063
Regional Division ∩ MPI	0.3636 ***	0.0017
Regional Division ∩ Slope	0.4375 **	0.0375
Grain for Green ∩ Temperature	0.5056 ***	0.0056
Grain for Green ∩ Precipitation	0.5044 ***	0.0037
Grain for Green ∩ MPI	0.3101 **	0.0101
Grain for Green ∩ Slope	0.2942 **	0.0100
Temperature ∩ Precipitation	0.6665 ***	0.0065
Temperature ∩ MPI	0.5717 *	0.0665
Temperature ∩ Slope	0.6337 **	0.0337
Precipitation ∩ MPI	0.4581 *	0.0581
Precipitation ∩ Slope	0.4859 *	0.0589
MPI ∩ Slope	0.2449 **	0.0449

Note: *** indicates significance at 0.01 level. ** indicates significance at 0.05 level. * indicates significance at 0.1 level.

Table 11. The dominant interactions between two covariates on greenness in 2020.

Interaction	Degree of the Relationship (q)	*p* Value
Regional Division ∩ Grain for Green	0.6568 ***	0.0058
Regional Division ∩ Temperature	0.5112 *	0.0812
Regional Division ∩ Precipitation	0.5038 ***	0.0038
Regional Division ∩ MPI	0.4491 **	0.0491
Regional Division ∩ Slope	0.4697 *	0.0697
Grain for Green ∩ Temperature	0.5535 ***	0.0035
Grain for Green ∩ Precipitation	0.5621 ***	0.0026
Grain for Green ∩ MPI	0.5165 **	0.0201
Grain for Green ∩ Slope	0.5455 ***	0.0045
Temperature ∩ Precipitation	0.5081 **	0.0208
Temperature ∩ MPI	0.4506 *	0.0550
Temperature ∩ Slope	0.4915 *	0.0591
Precipitation ∩ MPI	0.3747 **	0.0475
Precipitation ∩ Slope	0.3062 **	0.0474
MPI ∩ Slope	0.2864 **	0.0491

Note: *** indicates significance at 0.01 level. ** indicates significance at 0.05 level. * indicates significance at 0.1 level.

4. Discussion

4.1. Evaluation of the Interaction Between Ecology, Poverty, and Socio-Economic Development

In this study, we evaluated natural, poverty, and policy factors and their relationship with greenness for contiguous poverty-stricken areas in China. From 2000 to 2020, 59% of the area showed an increasing greenness trend, which means vegetation coverage changed for the better. Table 7 shows that the spatial autocorrelation of poverty status is gradually weakening, while Figure 6 indicates that the mutual influence between poverty status in neighboring areas is also weakening. There were more synergies with poverty alleviation in quick greening areas compared with stable and slow greening, which further proves that the greater the increase in greenness, the stronger the positive interaction between poverty alleviation and ecological environment protection (Figure 7). The natural factors, Grain for Green, and the intersection between regional division and natural factors have a great influence on greenness. Comparing 2000 and 2020, the impact of natural factors and poverty decreased, and the influence of the Grain for Green Policy increased. The fact that the Grain for Green interacted with poverty change was also influential.

The objective of this study was to obtain the greenness spatial–temporal change trend and poverty alleviation condition in contiguous poverty areas in China over the past twenty years and then explore the relationship between these two, as well as the influence of natural and human activities and policy on greenness. The BYM model analysis result of greenness showed the changing trend of greenness from 2000 to 2020, including in the whole area over time in Figure 3, as well as the spatial distribution in Figure 4. The change in the poverty condition was interpreted every 5 years from 2000 to 2020 by global and local spatial autocorrelation, as shown in the map of local Moran's I in Figure 6. The coupling method was applied to analyze the relationship between greenness and poverty in CPSAs. In this study, the concepts of synergy and trade-off were used to form different types of coupling relationships between the space–time changes in greenness and poverty, and the regional statistical results of 13 contiguous poverty-stricken areas and the mapping results of spatial distribution are obtained in Figure S3, which can demonstrate whether the greenness and poverty alleviation have the relationships of trade-off or synergy and their percentage in each region. The results of the Geodetector illustrated the impacts of factors and their interactive combination on greenness. Moreover, by comparing the two time periods, 2000 and 2020, we can see the changes in the impact of factors and their interactive combinations on greenness.

4.2. The Development of Policy Factors Has Changed the Effects of Natural Factors Affecting Vegetation Greenness

Previous work showed that global greening results mainly from CO_2, climate change, nitrogen deposition, and land cover [2]. However, these studies only analyzed natural influencing factors, and there are still unexplained parts in their results that may relate to human activities and policy. In this study, we added the Grain for Green Policy and poverty conditions to the factors group and obtained their impacts on greenness. But, according to the results of Geodetector modeling in Tables 8 and 9, MPI did not have a significant influence ($p > 0.05$); this may be because the settings for strata in Geodetector are poverty-stricken areas, which dominates and make the poverty characteristics consistent, i.e., there is not a difference in MPI to drive changes in greenness. Regarding the coupling of poverty and the environment, there were relevant studies that interpreted the framework between them [8], but there is a lack of country-level study from a whole strategic aspect. Results in Figure S3 show the coupling relationship between greenness and poverty change in different degrees, including the percentage of trade-off and synergy in each region, as well as their spatial distribution in the whole of China.

As a result of the spatial–temporal change in greenness, its trend from 2000 to 2020 rose with fluctuation, especially in the first 10 years with the smallest value, −37.39. The year 2010 is the end of the first round of Grain for Green Policy, and 2012 is the beginning of the second round (Figure 3). From the results of overall temporal change, the negative value in 2012 and 2013 may be the end of the first round and the state of greenness before the start of the second round; that is, the change in greenness decreased significantly after the policy was stopped, and there was a one-year lag effect, which may be the reason for the vegetation growth cycle. After 2013, there was a rapid positive increasing trend from −28.53 to 27.11.

4.3. Interpretation of the Synergistic Relationship Between Ecological Environment and Poverty to Varying Degrees

In the relationship between greenness change and poverty change, the proportion of trade-off (66.61%) is more than that of synergy (33.39%) (Figure S3). In cases of greenness growth, the proportion of synergy in greening areas is more than that in browning areas, which means that the greater the change degree and speed of greening, the stronger the synergy relationship between greening and poverty alleviation. It shows that greenness conditions and poverty alleviation are mutually reinforcing, which is also consistent with the theory that the improvement of vegetation and the ecological environment can improve the living environment. Further, Fisher and Genevieve [53] have shown that this improved

living environment is associated with poverty alleviation and the quality of life of the population in poor areas so as to promote poverty alleviation. Furthermore, the proportion of synergy in quick greening areas was larger than that in slow and stable greening areas. This may be due to the greening of the living environment not keeping up with the rapid changes in the social economy, especially the vegetation ecological restoration itself, which has a relatively slow cycle of its own. Therefore, it could not have obvious effects like the stable improvement of the environment. Furthermore, from the perspective of spatial distribution, poverty is closely intertwined with environmental and geographical conditions. The use of low-input agriculture in environmentally vulnerable areas like most areas of Xinjiang and the Qinghai–Tibet Plateau in Figure 7 leads to ecological degradation, such as land degradation; as a result, vegetation browning occurred, and poverty status has not improved. In some poverty areas, impoverished groups overly rely on environmental resources for survival, and local governments sometimes have to sacrifice the environment in pursuit of economic growth. However, in poverty-stricken areas with better ecological environments, such as some southwestern parts in Figure 7 with a positive greening trend, their poverty condition change did not follow its corresponding condition. This might be because some environmental protection measures there have not taken into account the development opportunities of the poor group, which limits people's access to natural resources and leads to further poverty in the area. Academia and government officials generally believe that there is a vicious cycle of poverty and ecological degradation, which is one of the main reasons for the slow socio-economic development in underdeveloped areas [53]. Therefore, we should fully recognize the inherent complexity between poverty and environmental issues, as well as the trade-offs, synergies, and mutual influences between these complex factors.

4.4. Novelty and Contribution

This paper contributes to the application of geographic information to ecology and poverty studies. We developed an innovative conceptual framework utilizing emerging geographical information scientific technologies, as well as models, to identify significant conclusions. This paper evaluated regional poverty from a geographical perspective, expanding from the household to its spatial agglomeration and providing intermittent observations of long time series. These are innovative and contributing research perspectives.

In summary, our findings reveal that the larger the increase in greenness, the more mutual promotion there is between poverty alleviation and the ecological environment, and conservation efforts enhance environmental outcomes and contribute to local poverty alleviation. These results have important implications for both local and broader policy-making. Local policymakers should prioritize integrating such human–land relationship mechanisms into regional management plans. By supporting community involvement in conservation, policies can address local ecological needs while also enhancing socio-economic benefits. Specifically, programs that empower local residents to participate in and benefit from conservation activities, like setting up other policies that are similar to the Grain for Green Policy according to local conditions and our results of the different coupling relationship percentages (Figure S3), could lead to more sustainable environmental practices and improved livelihoods. Local governments could benefit from designing targeted subsidies or incentives to encourage practices that simultaneously address ecological degradation and support poverty communities. For instance, promoting sustainable agroforestry systems could improve soil health and increase local farmers' income, thereby contributing to both environmental and economic sustainability in a positive human–land relationship. In the context of rural revitalization, these approaches can help align economic incentives with environmental goals, such as through the development of eco-tourism or sustainable agroforestry projects that benefit both the environment and local communities. At a broader level, our findings advocate for the integration of ecological protection measures with national poverty alleviation and even the current rural revitalization frameworks. This study highlights the need for national policies that promote a balanced approach, ensuring

that economic development does not come at the expense of environmental health. Such measures could create synergies between environmental protection and poverty alleviation efforts, ultimately fostering a more resilient and sustainable environment and society across China.

4.5. Limitations

In the application of methods, including Bayesian spatial–temporal models, Moran's I, LISA, and Geodetector model applied to ecological and poverty studies, several limitations and challenges need to be considered. The Bayesian spatial–temporal model is a tool that can effectively capture complex interactions between spatial and temporal variables, leveraging Bayesian inference to incorporate prior knowledge into the analysis. However, large datasets are required to generate reliable results. This computational demand can pose substantial barriers in resource-constrained settings or when working with sparse data.

Moran's I and the local indicator of spatial association (LISA) provide global and local measures of spatial autocorrelation, indicating the degree to which spatial units exhibit similar values in a geographic context. While it is useful for assessing spatial patterns, it offers limited exploration into temporal changes. For instance, they might detect spatial clustering and localized phenomena of environmental variables or poverty levels but cannot reveal temporal shifts, such as changes in local conditions or fluctuations in poverty rates over time. This is also the reason we undertook the spatial correlation study of poverty conditions every five years to obtain its changes. However, when it comes to nuanced dynamics that influence both ecological and socio-economic systems, this limitation would hinder the ability to interpret it.

The Geodetector model is effective for detecting spatial heterogeneity and examining the impact of various spatial factors on a particular outcome. It can identify spatial interactions and variations, but it is inherently limited by their lack of temporal integration. The Geodetector model can highlight spatial variations in ecological environment, land use, or economic development but fails to account for how these patterns change over time, potentially missing key temporal dynamics that influence ecological and socio-economic outcomes. This is also why we did a comparison between 2000 and 2020 to identify its changes.

The data used pose some limitations. We worked with county-level data, which can lead to some uncertainties in the analysis and interpretations, annual cumulative total precipitation, and annual mean temperature, losing more details of the county-level study unit. Despite these limitations, studies at the finer resolution are difficult to access and lack the spatial coverage that was achieved in our study. This would especially require a large number of field investigations with ethical authorities for households on a large scale, which would not be very feasible.

4.6. Future Directions

Our research here focused on the change in greenness in continuous poverty-stricken areas. We compared the poverty areas with the non-poverty areas, especially the effects of a series of ecological protection, restoration, and even ecological poverty alleviation policies specifically for the poverty areas. Based on the completion of the major task of targeted poverty alleviation in China, this series of related policy measures also came to an end when China announced its comprehensive poverty alleviation at the end of 2020. In the future, according to China's national strategy, the whole country will implement the rural revitalization strategy in accordance with the strategic deployment of the Party Central Committee and the State Council [54]. Therefore, looking forward to future research, we can start with the importance of ecology, analyze the status and role of ecological revitalization in rural revitalization, point out the current problems in rural areas main ecological issues, and propose corresponding strategic strategies and measures to make positive contributions to promoting rural ecological revitalization. Chinese scholars have conducted extensive research on ecological environmental indicators based on national, provincial, or

urban conditions. Most scholars construct relevant indicator systems based on ecological civilization construction [55]. Based on the rural situation, most scholars choose to study rural ecological environment governance or its performance evaluation. A few scholars have conducted research from the perspective of rural ecological civilization construction, and some scholars have conducted research and evaluations on rural ecological environment quality [56]. Overall, there is not much research on rural ecological revitalization in China, and most studies emphasize economic development too much, while ecological revitalization emphasizes better living conditions and healthy and stable ecosystems [57]. Based on this, future research can still rely on the use of Earth observation and remote sensing datasets, and new targeted characterization indicators and statistical data will be developed based on national policies and corresponding rural ecological revitalization policies in the future. In the meantime, after mastering the context of China, we can further compare the situation of other countries in the world. For example, in South America, countries like Brazil have huge tropical rainforests, and the local people rely on them for survival [58]. However, there are still intertwined issues of poverty and ecology. So, relative management and governance may also exist in countries with similar situations. In the future, comparing research on countries with such a global situation, and based on existing systematic research on China, should be considered to provide a more comprehensive and macro-global perspective to explore the issue of sustainable development in such a human–land relationship.

5. Conclusions

In the 13 CPSAs (contiguous poverty-stricken areas) in China, the increasing greenness change trend exists in 59% of study areas, as shown in Figure S2. Poverty status has improved from 2000 to 2020 (Figure 5). In 2000, the high poverty levels with larger MPIs were widely distributed. After 20 years, the overall MPI value was lower, except for some northwest regions with increased MPI values (Figure 5). The spatial autocorrelation and spatial pattern of poverty also changed, and the spatial autocorrelation shows a fluctuating trend of first rising and then falling overall, as shown in Table 7, and it showed the largest change around 2010. There were also some differences in the space distribution, and the mutual influence of poverty conditions in adjacent regions decreased (Figure 6). There were more synergies with poverty alleviation in quickly greening areas compared with stable and slowly greening areas, which can be evidence that the better the greenness, the more mutual promotion between poverty alleviation and ecological environment (Figure S3). In 2000, temperature and precipitation played positive roles in influencing greenness, followed closely by poverty division (Table 8). After 20 years, poverty division and Grain for Green Policy have taken the lead, with temperature and precipitation following in terms of their effect on greenness (Table 9). Compared with 2000 and 2020, the impact of natural factors, poverty regional division, and poverty level decreased, and the impact of the Grain for Green policy increased. The intersection between regional division and natural factors has great influence, as shown in Tables 10 and 11. In order to successfully balance sustainable development, policymaking and solutions should come from consideration of the ecological and environmental degradation and poverty taken together to achieve double-win strategies. We should pay more attention to making and implementing policies according to local conditions in order to maintain the human–land relationship with sustainability. According to the current results of our study, the proportion and spatial distribution of the synergistic relationship between the two vary in different regions. This result can serve as a reference to help policymakers coordinate the human–environment relationship. In the subsequent driving factor analysis, it can be found that natural factors are gradually influenced by long-term and large-scale policy implementation over a long period of time, so the importance of policy implementation has also been ranked as being at the forefront. Therefore, coordinating the overall human–environment relationship is also crucial for policymakers to carry out strategic planning at the national level.

Supplementary Materials: The following supporting information can be downloaded at https://www.mdpi.com/article/10.3390/rs16213938/s1. The Supplementary Materials contain the calculation and coding of Bayesian spatial–temporal modeling by OpenBUGS software and process figures. Figures include Figure S1: Image histograms generated by MODIS LAI values at a resolution of 500 m in all counties of CPSAs in the study area each year. The horizontal axis represents the range of LAI values, and the vertical axis represents the frequency. The unit of the vertical axis is 10^7. Figure S2: Proportion of greenness changes. Figure S3: Synergies and trade-offs percentage accumulation of the relationship between greenness change and poverty change in CPSAs and the relationship affected by browning, slowly greening, stable greening, and quick greening areas. Figure S4: Trace plots (first row), autocorrelation plots (second row), and the posterior densities (third row) for selected variables in Model 2 (b0 = overall slope; b1 = departure from the overall slope for county). Trace plots for all these variables show mixing, and the autocorrelation plots show no evidence of high autocorrelation for the chains.

Author Contributions: Conceptualization, W.X. and Y.G.; formal analysis, W.X. and N.A.S.H.; methodology, W.X. and N.A.S.H.; supervision, Y.G., N.A.S.H. and G.M.F.; writing—original draft, W.X.; writing—review and editing, W.X., Y.G., N.A.S.H., G.M.F. and Z.R. All authors have read and agreed to the published version of the manuscript.

Funding: This research is supported by the National Natural Science Foundation of China (Grant No. 42230110). Wentong Xie is supported by a Ph.D. scholarship from the University of Nottingham Ningbo, China, as part of a doctoral training partnership with the Institute for Geographic Science and Natural Resources Research (IGSNRR), CAS.

Data Availability Statement: Dataset available on request from the authors.

Conflicts of Interest: The authors declare no conflicts of interest.

References

1. UNDP. *The Millennium Development Goals Report 2015*; UNDP: New York, NY, USA, 2015; pp. 155–157.
2. Zhu, Z.; Piao, S.; Myneni, R.B.; Huang, M.; Zeng, Z.; Canadell, J.G.; Ciais, P.; Sitch, S.; Friedlingstein, P.; Arneth, A.; et al. Greening of the Earth and its drivers. *Nat. Clim. Chang.* **2016**, *6*, 791–795. [CrossRef]
3. Piao, S.; Wang, X.; Park, T.; Chen, C.; Lian, X.; He, H.; Bjerke, J.; Chen, A.; Ciais, P.; Tømmervik, H.; et al. Characteristics, drivers and feedbacks of global greening. *Nat. Rev. Earth Environ.* **2019**, *1*, 14–27. [CrossRef]
4. Chen, C.; Park, T.; Wang, X.; Piao, S.; Xu, B.; Chaturvedi, R.K.; Fuchs, R.; Brovkin, V.; Ciais, P.; Fensholt, R.; et al. China and India lead in greening of the world through land-use management. *Nat. Sustain.* **2019**, *2*, 122–129. [CrossRef]
5. Cheng, X.; Shuai, C.; Liu, J.; Wang, J.; Liu, Y.; Li, W.; Shuai, J. Topic modelling of ecology, environment and poverty nexus: An integrated framework. *Agric. Ecosyst. Environ.* **2018**, *267*, 1–14. [CrossRef]
6. Cavendish, W. Empirical Regularities in the Poverty-Environment Relationship of Rural Households: Evidence from Zimbabwe. *World Dev.* **2000**, *28*, 1979–2003. [CrossRef]
7. Casillas, C.E.; Kammen, D.M. The Energy-Poverty-Climate Nexus. *Science* **2010**, *330*, 1181–1182. [CrossRef] [PubMed]
8. Shuai, J.; Cheng, X.; Tao, X.; Shuai, C.; Wang, B. A Theoretical Framework for Understanding the Spatial Coupling between Poverty and the Environment: A Case Study from China. *Agron. J.* **2019**, *111*, 1097–1108. [CrossRef]
9. Chris, D. The ecology of rural poverty. *Nat. Ecol. Evol.* **2017**, *1*, 1060–1061. [CrossRef]
10. Liu, J.G.; Li, S.X.; Ouyang, Z.Y.; Tam, C.; Chen, X.D. Ecological and socioeconomic effects of China's policies for ecosystem services. *Proc. Nat. Acad. Sci. USA* **2008**, *105*, 9477–9482. [CrossRef]
11. Feng, Z.M.; Yang, Y.Z.; Zhang, Y.Q.; Zhang, P.T.; Li, Y.Q. Grain-for-green policy and its impacts on grain supply in West China. *Land Use Policy* **2005**, *22*, 301–312. [CrossRef]
12. The State Council of China. Outline for Developmentoriented Poverty Reduction for China's Rural Areas (2011–2020). Available online: http://www.gov.cn/gongbao/content/2011/content_2020905.htm (accessed on 2 May 2020).
13. Zhou, Y.; Liu, Y. The geography of poverty: Review and research prospects. *J. Rural. Stud.* **2022**, *93*, 408–416. [CrossRef]
14. Zheng, Y.; Lin, T.; Hamm, N.A.S.; Liu, J.; Zhou, T.; Geng, H.; Zhang, J.; Ye, H.; Zhang, G.; Wang, X.; et al. Quantitative evaluation of urban green exposure and its impact on human health: A case study on the 3-30-300 green space rule. *Sci. Total Environ.* **2024**, *924*, 171461. [CrossRef] [PubMed]
15. Dempsey, C. The Gray-Green Urban Divide: How Wealth and Poverty Are Visible from Space. Available online: https://www.geographyrealm.com/gray-green-urban-divide-wealth-poverty-visible-space/ (accessed on 3 August 2016).
16. Zhang, Y.; Song, C.; Band, L.E.; Sun, G.; Li, J. Reanalysis of global terrestrial vegetation trends from MODIS products: Browning or greening? *Remote Sens. Environ.* **2017**, *191*, 145–155. [CrossRef]
17. Alexandridis, T.; Ovakoglou, G.; Clevers, J.G.P.W. Relationship between MODIS EVI and LAI across time and space. *Geocarto Int.* **2019**, *35*, 1385–1399. [CrossRef]

18. Zhao, S.; Wu, X.; Zhou, J.; Pereira, P. Spatiotemporal tradeoffs and synergies in vegetation vitality and poverty transition in rocky desertification area. *Sci. Total Environ.* **2021**, *752*, 141770. [CrossRef]
19. Holland, E.A.; Braswell, B.H.; Sulzman, J.; Lamarque, J.F. Nitrogen deposition onto the United States and western Europe: Synthesis of observations and models. *Ecol. Appl.* **2005**, *15*, 38–57. [CrossRef]
20. Ord, K.; Getis, A. Local Spatial Autocorrelation Statistics: Distributional Issues and an Application. *Geogr. Anal.* **2010**, *27*, 286–306. [CrossRef]
21. Odongo, V.; Hamm, N.; Milton, E. Spatio-Temporal Assessment of Tuz Gölü, Turkey as a Potential Radiometric Vicarious Calibration Site. *Remote Sens.* **2014**, *6*, 2494–2513. [CrossRef]
22. Ge, Y.; Hu, S.; Ren, Z.; Jia, Y.; Wang, J.; Liu, M.; Zhang, D.; Zhao, W.; Luo, Y.; Fu, Y.; et al. Mapping annual land use changes in China's poverty-stricken areas from 2013 to 2018. *Remote Sens. Environ.* **2019**, *232*, 111285. [CrossRef]
23. Wang, J.; Zhang, T.; Fu, B. A measure of spatial stratified heterogeneity. *Ecol. Indic.* **2016**, *67*, 250–256. [CrossRef]
24. Zuo, C.S. *Evolution of China's Poverty Alleviation and Development Policy (2001–2015)*; Zuo, C., Ed.; Springer: Singapore, 2016; Volume 16–18, p. 315.
25. Qiwei, C.; Kangning, X.; Wenhong, D.; Lianlian, N. Coupling characteristics of ecological and poverty in typical karst area: Case study of 9000 provincial level poor villages in Guizhou Province. *Acta Ecol. Sin.* **2021**, *41*, 2968–2982. [CrossRef]
26. The State Council of the People's Republic of China. National Main Functional Area Planning. Available online: http://www.gov.cn/zhengce/2020-06/11/content_5518767.htm (accessed on 11 June 2020).
27. Reuter, H.I.; Nelson, A.; Jarvis, A. An evaluation of void-filling interpolation methods for SRTM data. *Int. J. Geog. Inf. Sci.* **2007**, *21*, 983–1008. [CrossRef]
28. Xu, X.L.; Liu, J.Y.; Zhang, S.W.; Li, R.D.; Yan, C.Z.; Wu, S.X. China's Multi-Period Land Use Land Cover Remote Sensing Monitoring Dataset (CNLUCC). 2018. Available online: https://www.resdc.cn/DOI/doi.aspx?DOIid=54 (accessed on 10 November 2021).
29. Myneni, R.; Knyazikhin, Y.; Park, T. MOD15A3H MODIS/Combined Terra+Aqua Leaf Area Index/FPAR Daily L4 Global 500m SIN Grid. 2015. Available online: https://ladsweb.modaps.eosdis.nasa.gov/missions-and-measurements/products/MCD15A3H (accessed on 4 September 2021).
30. Xu, X. Annual Spatial Interpolation Datasets of Meteorological Elements in China. Available online: https://www.resdc.cn/DOI/doi.aspx?DOIid=96 (accessed on 10 November 2021).
31. The National Aeronautics and Space Administration (NASA) and the National Geospatial-Intelligence Agency (NGA). USGS EROS Archive—Digital Elevation—Shuttle Radar Topography Mission (SRTM) 1 Arc-Second Global. 2000. Available online: https://cmr.earthdata.nasa.gov/search/concepts/C1220567890-USGS_LTA.html (accessed on 10 November 2021).
32. NASA and Japan's Ministry of Economy, Trade and Industry (METI). ASTER's Global Digital Elevation Model (GDEM). 2009. Available online: https://www.jpl.nasa.gov/images/pia12090-asters-global-digital-elevation-model-gdem/ (accessed on 10 February 2022).
33. The European Space Agency. Copernicus DEM—Global and European Digital Elevation Model (COP-DEM). 2019. Available online: https://dataspace.copernicus.eu/explore-data/data-collections/copernicus-contributing-missions/collections-description/COP-DEM (accessed on 18 February 2022).
34. National Aeronautics and Space Administration; Jet Propulsion Laboratory; California Institute of Technology. NASADEM. 2020. Available online: https://lpdaac.usgs.gov/documents/592/NASADEM_User_Guide_V1.pdf (accessed on 10 February 2022).
35. Besag, J.; York, J.; Mollié, A. Bayesian image restoration, with two applications in spatial statistics. *AnISM* **1991**, *43*, 1–20. [CrossRef]
36. Garson, G.D. Fundamentals of Hierarchical Linear and Multilevel Modeling. In *Hierarchical Linear Modeling: Guide and Applications*; Sage Publications, Inc.: Sauzendoaks, CA, USA, 2013. [CrossRef]
37. Haining, R. *Spatial Data Analysis. Theory and Practice*; Cambridge University Press: Cambridge, UK, 2004.
38. Li, G.; Haining, R.; Richardson, S.; Best, N. Space–time variability in burglary risk: A Bayesian spatio-temporal modelling approach. *Spat. Stat.* **2014**, *9*, 180–191. [CrossRef]
39. Lunn, D.J.; Thomas, A.; Best, N.; Spiegelhalter, D. WinBUGS—A Bayesian modelling framework: Concepts, structure, and extensibility. *Stat. Comput.* **2000**, *10*, 325–337. [CrossRef]
40. UNDP. *Human Development Report 2010—20th Anniversary Edition; The Real Wealth of Nations: Pathways to Human Development*; UNDP: New York, NY, USA, 2010.
41. Wagle, U. Multidimensional Poverty Measurement with Economic Well-being, Capability, and Social Inclusion: A Case from Kathmandu, Nepal. *J. Hum. Dev.* **2005**, *6*, 301–328. [CrossRef]
42. Deutsch, J.; Silber, J. Measuring Multidimensional Poverty: An Emperical Comparision of Various Approches. *Rev. Income Wealth* **2005**, *51*, 145–174. [CrossRef]
43. Liu, Q.; Yang, X.; Shi, Y.; Chen, J.; Lu, D. Assessment of Livelihood Security Based on DPSIR Model in Concentrated Destitute Area of Liupan Mountains. *Mt. Res.* **2018**, *36*, 11. [CrossRef]
44. Cheng, X.; Guo, Q.; Liao, H.; He, T.; Liu, Y.; Zhu, L. Study on Multidimensional Poverty Measurement and the Migration Path of Poverty Focus in Counties—A case study of Wuling Mountain Region of Chongqing. *J. Northwest Univ. (Nat. Sci. Ed.)* **2021**, *43*, 1–9. [CrossRef]
45. Schabenberger, O.; Gotway, C.A. *Statistical Methods for Spatial Data Analysis*; Chapman and Hall/CRC: New York, NY, USA, 2005.

46. Xiong, G.; Cao, X.; Hamm, N.A.S.; Lin, T.; Zhang, G.; Chen, B. Unbalanced Development Characteristics and Driving Mechanisms of Regional Urban Spatial Form: A Case Study of Jiangsu Province, China. *Sustainability* **2021**, *13*, 3121. [CrossRef]
47. Rey, S.J.; Janikas, M.V. STARS: Space-time analysis of regional systems. *Geogr. Anal.* **2006**, *38*, 67–86. [CrossRef]
48. Liu, Y.; Lü, Y.; Fu, B.; Harris, P.; Wu, L. Quantifying the spatio-temporal drivers of planned vegetation restoration on ecosystem services at a regional scale. *Sci. Total Environ.* **2019**, *650*, 1029–1040. [CrossRef]
49. Chen, H.; Marter-Kenyon, J.; López-Carr, D.; Liang, X.Y. Land cover and landscape changes in Shaanxi Province during China's Grain for Green Program (2000–2010). *Environ. Monit. Assess.* **2015**, *187*, 644. [CrossRef] [PubMed]
50. Zhang, R.Q.; Tang, C.J.; Ma, S.H.; Yuan, H.; Gao, L.L.; Fan, W.Y. Using Markov chains to analyze changes in wetland trends in arid Yinchuan Plain, China. *Math. Comput. Modell.* **2011**, *54*, 924–930. [CrossRef]
51. National Forestry and Grassland Administration. Notice on Further Improving Policy Measures to Consolidate the Achievements of Grain to Green Policy. Available online: https://www.forestry.gov.cn/search/76653 (accessed on 28 October 2022).
52. Wang, J.; Wang, K.L.; Zhang, M.Y.; Zhang, C.H. Impacts of climate change and human activities on vegetation cover in hilly southern China. *Ecol. Eng.* **2015**, *81*, 451–461. [CrossRef]
53. Fisher, J.A.; Patenaude, G.; Giri, K.; Lewis, K.; Meir, P.; Pinho, P.; Rounsevell, M.D.A.; Williams, M. Understanding the relationships between ecosystem services and poverty alleviation: A conceptual framework. *Ecosyst. Serv.* **2014**, *7*, 34–45. [CrossRef]
54. Wang, X.; Wu, J.; Jiang, H. Dynamic Assessment and Trend Prediction of Rural Eco-environmental Quality in China. *J. Nat. Resour.* **2017**, *32*, 864–876.
55. Huang, G. A look at rural ecological revitalization. *Chin. J. Eco-Agric.* **2019**, *27*, 190–197. [CrossRef]
56. Yuju, W. A Critical View on the Status Quo of the Farmland Soil Environmental Quality in China: Discussion and Suggestion of Relevant Issues on Report on the national general survey of soil contamination. *J. Agro-Environ. Sci.* **2014**, *33*, 1465–1473. [CrossRef]
57. Ma, X.; Hua, Y. Establishing an Evaluation Index System for Measuring the Effect of Rural Ecological Revitalization. *J. China Agric. Resour. Reg. Plan.* **2021**, *42*, 60–67. [CrossRef]
58. Pinho, P.F.; Patenaude, G.; Ometto, J.P.; Meir, P.; Toledo, P.M.; Coelho, A.; Young, C.E.F. Ecosystem protection and poverty alleviation in the tropics: Perspective from a historical evolution of policy-making in the Brazilian Amazon. *Ecosyst. Serv.* **2014**, *8*, 97–109. [CrossRef]